

RESEARCH

Open Access



New bakuchiol dimers from *Psoraleae Fructus* and their inhibitory activities on nitric oxide production

Qingxia Xu[†], Qian Lv[†], Lu Liu, Yingtao Zhang^{*} and Xiuwei Yang^{*}

Abstract

Background: Dried fruits of *Psoralea corylifolia* L. (*Psoraleae Fructus*) is one of the most popular traditional Chinese medicine with treatment for nephritis, spermatorrhea, pollakiuria, asthma, and various inflammatory diseases. Bakuchiol is main meroterpenoid with bioactive diversity from *Psoraleae Fructus*. This study was designed to seek structural diverse bakuchiol derivants with anti-inflammatory activities from this plant.

Methods: Various column chromatography methods were used for isolation experiment. Structures and configurations of these compounds were determined by spectroscopic methods and single-crystal X-ray diffraction. Their inhibition on nitric oxide (NO) production in lipopolysaccharide (LPS)-stimulated RAW264.7 macrophages were evaluated by the Griess reaction.

Results: Twelve unrepresented bakuchiol dimmers, bisbakuchiols M–U (1–9) and bisbakuchiol ethers A–C (10–12), along with five known compounds (13–17), were isolated from the fruits of *Psoralea corylifolia* L. Compounds 1–3, 10–12, 16 and 17 exhibited inhibitory activities against LPS-induced NO production in RAW264.7 macrophages, and the inhibition of compound 1 (half maximal inhibitory concentration (IC₅₀) value = 11.47 ± 1.57 μM) was equal to that of L-N(6)-(1-iminoethyl)-lysine (IC₅₀ = 10.29 ± 1.10 μM) as a positive control.

Conclusions: Some compounds exhibited inhibitory activities against NO production, and the study of structure–activity relationship suggested that uncyclized compounds with oxygen substitution at C-12/12' showed strong inhibitory activities, and carbonyl units contributed to enhanced activities.

Keywords: *Psoralea corylifolia*, bakuchiol dimers, Inhibition of nitric oxide

Background

The higher plant, *Psoralea corylifolia* L. (*Cullen corylifolia* (L.) Mefik) is an annual herb and belongs to family Leguminosae, distributed in China, India, Malay peninsula, and Indonesia [1]. Dried fruits of *P. corylifolia*

(*Psoraleae Fructus*) is one of the most popular traditional Chinese medicine (TCM) and officially listed in Chinese Pharmacopoeia [2], and it is also a natural food additive [3]. It has been used for the treatment of nephritis, spermatorrhea, pollakiuria, asthma, and various inflammatory diseases [4]. *Psoraleae Fructus* contains approximately 110 compounds including coumarins, flavonoids, meroterpenoids, and benzofurans [5]. Among these, meroterpenoids are considered to be the one of characteristic and active components [6, 7].

Bakuchiol is a main meroterpenoid that consists of a side chain (3-ethenyl-3,7-dimethyl-1,6-octadienyl) and a *p*-disubstituted benzene ring. Structural changes

*Correspondence: zytao@bjmu.edu.cn; xwyang@bjmu.edu.cn
[†]Qingxia Xu and Qian Lv are co-first authors and contributed equally to this work

State Key Laboratory of Natural and Biomimetic Drugs, Department of Natural Medicines, School of Pharmaceutical Sciences, Peking University Health Science Center, Peking University, No. 38, Xueyuan Road, Haidian District, Beijing 100191, China



© The Author(s) 2021. **Open Access** This article is licensed under a Creative Commons Attribution 4.0 International License, which permits use, sharing, adaptation, distribution and reproduction in any medium or format, as long as you give appropriate credit to the original author(s) and the source, provide a link to the Creative Commons licence, and indicate if changes were made. The images or other third party material in this article are included in the article's Creative Commons licence, unless indicated otherwise in a credit line to the material. If material is not included in the article's Creative Commons licence and your intended use is not permitted by statutory regulation or exceeds the permitted use, you will need to obtain permission directly from the copyright holder. To view a copy of this licence, visit <http://creativecommons.org/licenses/by/4.0/>. The Creative Commons Public Domain Dedication waiver (<http://creativecommons.org/publicdomain/zero/1.0/>) applies to the data made available in this article, unless otherwise stated in a credit line to the data.

including oxidation, dehydration reduction, condensation and alkylation, occur in the side chain and benzene ring, which increases structural and bioactive diversities of meroterpenoid constituents. Remarkably, bakuchiol and its' derivants exhibited extensive bioactivities, such as anti-inflammatory, anti-oxidant, antitumor, anti-depressant, antidiabetic and osteoblastic activities [8]. Therefore, people have been trying to find monoterpenes with various biological activities. According to predecessors' researches, 22 meroterpenoids and 12 bakuchiol dimers were found from the plant [5, 9–11]. In our previous researches [12, 13], fourteen meroterpenoids and seventeen heterodimers of bakuchiol have been reported and their anticancer cytotoxicity were evaluated. Further investigation on the cyclohexane extract brought about twelve unrepresented bakuchiol dimmers, bisbakuchiols M–U (1–9) and bisbakuchiol ethers A–C (10–12), along with five known compounds (13–17), whose anti-inflammatory activities were evaluated. Herein structure elucidation of these compounds and evaluation of their ability to inhibit nitric oxide (NO) production in lipopolysaccharide (LPS)-stimulated RAW264.7 macrophages were discussed.

Materials and methods

General experimental procedures

Infrared data were recorded on a Thermo Nicolet Nexus 470 FT-IR spectrometer. Ultraviolet data were acquired on a Mapada UV-6100 double beam spectrophotometer. HRESIMS data were collected using a Waters Xevo G2 QTOF spectrometer. NMR spectra were recorded on a Bruker AVANCE III HD 400 NMR spectrometer. Optical rotations were measured on a Rudolph Autopol IV automatic polarimeter. X-ray data were collected by a Rigaku Micromax-003 X-ray single-crystal diffractometer with CuK α radiation. Open column chromatography (CC) was performed by packing silica gel (200–300 mesh, Marine Chemical Ltd., Qingdao, China), Sephadex LH-20 gel (Pharmacia Biotek, Denmark). Thin layer chromatography (TLC) was carried out on silica gel GF254 plates (Merck, Darmstadt, Germany) with 10% H₂SO₄ in 95% ethanol followed by heating. Reversed phase semi-preparative HPLC (RP-SP-HPLC) was accomplished using an LC3000 system (Beijing Innovation Technology Co., Ltd), equipped with a phenomenon C₁₈ column (21.2 mm \times 250 mm, 5 μ m). Cells were cultured in Sanyo MCO-15 AC carbon dioxide (CO₂) incubator (Sanyo Electric Co., Ltd., Osaka, Japan).

HPLC grade solvents, methanol (MeOH) and acetonitrile (MeCN), were purchased from Fisher Scientific (Pittsburgh, PA, USA) and solvents, petroleum ether (PE), cyclohexane (cHE), ethyl acetate (EtOAc), chloroform (CHCl₃) and normal-butanol (BuOH) for

column chromatography purchased from Beijing Chemical Works (Beijing, China). Dulbecco's modified Eagle's medium (DMEM), fetal bovine serum (FBS), trypsin, penicillin–streptomycin solution, phosphate buffered saline were obtained from Gibco® (Life Technologies Inc., Grand Island, NY, USA). 3-(4,5-Dimethyl-2-thiazolyl)-2,5-diphenyl-2H-tetrazolium bromide (MTT), lipopolysaccharide (LPS), Griess reagent, dimethylsulfoxide (DMSO), and L-N(6)-(1-iminoethyl)-lysine (L-NIL) were obtained from Sigma-Aldrich (St. Louis, MO, USA). The murine macrophage cell line RAW264.7 was obtained from the Cell Bank of the Chinese Academy of Sciences (Shanghai, China).

Plant material

The mature fruits of *Psoralea corylifolia* L. were harvested from Yunnan province of People's Republic of China (GPS coordinates:23°32'N, 99°23'E) in October 2016, and authenticated by Prof. Xiu-Wei Yang of the School of Pharmaceutical Sciences, Peking University. A voucher specimen (accession number: BGZ201610) of the fruits was deposited at the State Key Laboratory of Natural Medicines and Biomimetic Drugs of Peking University.

Extraction and isolation

The dried mature fruits powder (47.9 kg) was extracted with 70% aqueous ethanol under reflux. After extracted for three times (first 479 kg for 2 h, and then 384 kg for 2 h two times), the crude extract (8.2 kg, yield 17.12%) was obtained. And then, part of the residue (6.0 kg) was suspended in H₂O (8 L) and extracted with cHE (8 L \times 8), EtOAc (8 L \times 8) and *n*-butanol (BuOH, 8 L \times 8) successively and afforded corresponding extract for 1.2 kg, 2.2 kg and 0.7 kg. The cHE extract (1.0 kg) was fractionated by silica gel column (SGC, 140 mm i.d. \times 800 mm) with gradient eluent (PE-EtOAc, 5:1, 3:1, 1:1, 2:3, 1:3, 0:1, ν/ν) to give 26 fractions (Fr. A–Z). The Fr. B (27.2 g) was separated by SGC (55 mm i.d. \times 650 mm) with a step gradient eluent of PE-EtOAc (100: 1, 50: 1, 25: 1, 7: 1, 5: 1, 3:1, 1: 1, 1:3, 0:1, ν/ν) to afford 15 subfractions (Fr. B-1–Fr. B-15). Fr. B-8 (2.1 g) was separated by reversed-phase column (RPC), eluted with MeCN-H₂O (40:60 to 100:0, ν/ν), to give 13 subfractions. Fr. B-8-5 was purified by SP-RP-HPLC (MeCN-H₂O, 95:5, ν/ν), to yield compound **10** (5 mg, t_R =85 min). The Fr. C (136 g) was separated by SGC (120 mm i.d. \times 600 mm) with a step gradient eluent of PE-EtOAc (100: 1, 50: 1, 20: 1, 15: 1, 10: 1, 5:1, 5: 2, 1:1, 0:1, ν/ν) to afford 16 subfractions (Fr. C-1–Fr. C-16). Fr. C-4–7 was separated by Sephadex LH-20 column (SC) and purified by SP-RP-HPLC (MeCN-H₂O, 93:7, ν/ν), to yield compound **1** (230 mg, t_R =45 min) and **11** (60 mg, t_R =80 min). Fr. C-5 (20 g) was separated by RPC, eluted

with MeOH-H₂O (80:20 to 100:0, v/v), to give 9 subfractions. Fr.C-5-9 was separated by SC and purified by SP-RP-HPLC (MeCN-H₂O, 93:7, v/v), to yield compound **12** (34 mg, $t_R=71$ min). By SP-RP-HPLC (MeCN-H₂O, 90:10, v/v) and preparative TLC (PE-CHCl₃, 10:1, v/v), compound **2** (104 mg, $t_R=252$ min) was obtained from Fr. C-11 (2.1 g). The Fr. D (335 g) was separated by SGC (140 mm i.d. \times 800 mm) with a step gradient eluent of PE-CHCl₃ (100: 1, 50: 1, 20: 1, 10: 1, 5: 1, 4:1, 3: 1, 2: 1, 1: 1, 1:3, 0:100, v/v) to afford 14 subfractions (Fr. D-1-Fr. D-14). Fr. D-4 (20.7 g) was separated by RPC, eluted with MeOH-H₂O (45:55 to 100:0, v/v), to give 13 subfractions. Fr. D-4-12 was purified by SP-RP-HPLC (MeOH-H₂O, 93:7, v/v), to yield compounds **8** (15 mg, $t_R=131$ min) and **9** (28 mg, $t_R=136$ min). By SP-RP-HPLC (MeCN-H₂O, 90:10, v/v), Fr. D-7(1.7 g) was separated to yield compounds **3** (5 mg, $t_R=95$ min) and **4** (2 mg, $t_R=87$ min). The Fr. D-9 (37 g) was separated by SGC (55 mm i.d. \times 650 mm) with a step gradient eluent of PE-CHCl₃ (100: 1, 50: 1, 20: 1, 10: 1, 9: 1, 8:1, 7: 1, 6: 1, 5: 1, 4:1, 3:1, 1:1, 1:3, 0:1, v/v) to afford 28 subfractions. By SP-RP-HPLC (MeOH-H₂O, 92:8, v/v), Fr. D-9-13 was separated to yield compounds **5** (11 mg, $t_R=77$ min), **6** (9 mg, $t_R=100$ min) and **7** (19 mg, $t_R=110$ min). Fr. D-9-25 was purified by SP-RP-HPLC (MeOH-H₂O, 92:8, v/v), to give compounds **13** (18 mg, $t_R=86$ min) and **14** (25 mg, $t_R=92$ min). Fr. D-9-26 was purified by SP-RP-HPLC (MeOH-H₂O, 92:8, v/v), to give compound **15** (15 mg, $t_R=76$ min). Fr. D-11 (19.2 g) was separated by RPC, eluted with MeOH-H₂O (45:55 to 100:0, v/v), to give 27 subfractions. The Fr. D-11-25 (5.9 g) was separated by SGC (35 mm i.d. \times 500 mm) with a step gradient eluent of PE-CHCl₃ (8:1, 7: 1, 6: 1, 5: 1, 4:1, 3:1, 1:1, 1:3, 0:100, v/v) to afford 18 subfractions. By SP-RP-HPLC (MeOH-H₂O, 75:25, v/v), Fr. D-11-25-12 was separated to yield compounds **16** (14 mg, $t_R=286$ min) and **17** (15 mg, $t_R=328$ min).

Bisbakuchiol M (1). Brown-red needle crystals; mp 114-116 °C; $[\alpha]_{25}^D +50.0$ (c 0.1, MeOH); UV (MeOH) λ_{\max} (log ϵ): 204 (4.85), 258 (4.80), 386 (4.28) nm; IR (KBr) ν_{\max} 3315, 2967, 2930, 1692, 1609, 1582, 1504, 1385, 1358, 1255, 1035 cm⁻¹; ¹H NMR (CDCl₃, 400 MHz), see Table 1; ¹³C NMR (CDCl₃, 100 MHz), see Table 2; HRESIMS m/z 537.3004 [M+H]⁺ (calcd for C₃₆H₄₁O₄, 537.3005).

Bisbakuchiol N (2). Yellow oils; $[\alpha]_{25}^D +20.0$ (c 0.1, MeOH); UV (MeOH) λ_{\max} (log ϵ): 203 (4.41), 253 (4.44) nm; IR (KBr) ν_{\max} 3319, 2966, 2924, 1703, 1633, 1603, 1496, 1409, 1373, 1231, 969 cm⁻¹; ¹H NMR (CDCl₃, 400 MHz), see Table 1; ¹³C NMR (CDCl₃, 100 MHz), see Table 2; HRESIMS m/z 511.3573 [M+H]⁺ (calcd for C₃₆H₄₇O₂, 511.3576).

Bisbakuchiol O (3). Yellowish oils; $[\alpha]_{25}^D +30.0$ (c 0.1, MeOH); UV (MeOH) λ_{\max} (log ϵ): 203 (4.57), 267 (4.33) nm; IR (KBr) ν_{\max} 3373, 2962, 2926, 1704, 1604, 1507, 1454, 1372, 1238, 1172, 1007 cm⁻¹; ¹H NMR (CDCl₃, 400 MHz), see Table 1; ¹³C NMR (CDCl₃, 100 MHz), see Table 2; HRESIMS m/z 555.3468 [M+HCOO]⁻ (calcd for C₃₇H₄₇O₄, 555.3474).

Bisbakuchiol P (4). Yellowish oils; $[\alpha]_{25}^D -26.7$ (c 0.1, MeOH); UV (MeOH) λ_{\max} (log ϵ): 202 (4.61), 267 (4.32) nm; IR (KBr) ν_{\max} 3381, 2968, 2927, 1703, 1604, 1507, 1452, 1375, 1240, 1172, 1000 cm⁻¹; ¹H NMR (CDCl₃, 400 MHz), see Table 1; ¹³C NMR (CDCl₃, 100 MHz), see Table 2; HRESIMS m/z 509.3417 [M-H]⁻ (calcd for C₃₆H₄₅O₂, 509.3420).

Bisbakuchiol Q (5). Yellowish oils; $[\alpha]_{25}^D +70.0$ (c 0.1, MeOH); UV (MeOH) λ_{\max} (log ϵ): 202 (4.76), 264 (4.55) nm; IR (KBr) ν_{\max} 3370, 2964, 2921, 1704, 1607, 1507, 1459, 1370, 1238, 1171, 1099 cm⁻¹; ¹H NMR (CDCl₃, 400 MHz), see Table 1; ¹³C NMR (CDCl₃, 100 MHz), see Table 2; HRESIMS m/z 525.3364 [M-H]⁻ (calcd for C₃₆H₄₅O₃, 525.3369).

Bisbakuchiol R (6). White amorphous powder; $[\alpha]_{25}^D +70.0$ (c 0.1, MeOH); UV (MeOH) λ_{\max} (log ϵ): 203 (4.57), 260 (4.35) nm; IR (KBr) ν_{\max} 3372, 2967, 2924, 1704, 1613, 1506, 1451, 1365, 1253, 1143, 1094 cm⁻¹; ¹H NMR (CDCl₃, 400 MHz), see Table 1; ¹³C NMR (CDCl₃, 100 MHz), see Table 2; HRESIMS m/z 603.3676 [M+HCOO]⁻ (calcd for C₃₈H₅₁O₆, 603.3686).

Bisbakuchiol S (7). White amorphous powders; $[\alpha]_{25}^D +60.0$ (c 0.1, MeOH); UV (MeOH) λ_{\max} (log ϵ): 204 (4.42), 260 (4.32) nm; IR (KBr) ν_{\max} 3373, 2968, 2925, 1705, 1614, 1506, 1450, 1364, 1235, 1143, 1082 cm⁻¹; ¹H NMR (CDCl₃, 400 MHz), see Table 1; ¹³C NMR (CDCl₃, 100 MHz), see Table 2; HRESIMS m/z 557.3635 [M-H]⁻ (calcd for C₃₇H₄₉O₄, 557.3631).

Bisbakuchiol T (8). Yellowish oils; $[\alpha]_{25}^D -20.0$ (c 0.1, MeOH); UV (MeOH) λ_{\max} (log ϵ): 202 (4.68), 222 (4.57), 262 (4.33) nm; IR (KBr) ν_{\max} 3395, 2967, 2921, 1702, 1588, 1507, 1450, 1375, 1267, 1171, 1010 cm⁻¹; ¹H NMR (CDCl₃, 400 MHz), see Table 1; ¹³C NMR (CDCl₃, 100 MHz), see Table 2; HRESIMS m/z 525.3367 [M-H]⁻ (calcd for C₃₆H₄₅O₃, 525.3369).

Bisbakuchiol U (9). Yellowish oils; $[\alpha]_{25}^D +20.0$ (c 0.1, MeOH); UV (MeOH) λ_{\max} (log ϵ): 202 (4.63), 265 (4.21) nm; IR (KBr) ν_{\max} 3387, 2966, 2922, 1703, 1587, 1507, 1451, 1374, 1267, 1171, 1009 cm⁻¹; ¹H NMR (CDCl₃, 400 MHz), see Table 1; ¹³C NMR (CDCl₃, 100 MHz), see Table 2; HRESIMS m/z 525.3371 [M-H]⁻ (calcd for C₃₆H₄₅O₃, 525.3369).

Bakuchiol ether A (10). Yellowish oils; $[\alpha]_{25}^D +10.0$ (c 0.1, MeOH); UV (MeOH) λ_{\max} (log ϵ): 204(4.26),260(4.15) nm; IR (KBr) ν_{\max} 3424, 2969, 2929, 1712, 1603, 1505, 1453, 1369, 1224, 1136, 913 cm⁻¹; ¹H NMR (CDCl₃,

Table 1 ^1H NMR (400 MHz, CDCl_3 ; δ_{H} , J in Hz) data for compounds 1–9

Position	1	2	3	4	5	6	7	8	9
1									
2	7.42 (d, 8.6)	7.26 (d, 2.4)	7.00 (d, 8.6)	6.96 (d, 8.7)	7.17 (d, 8.4)	7.19 (d, 8.6)	7.21 (d, 8.5)	6.93 (br s)	6.92 (br s)
3	7.04 (d, 8.6)		6.43 (d, 8.6)	6.36 (d, 8.7)	6.72 (d, 8.4)	6.72 (d, 8.6)	6.79 (d, 8.5)		
4									
5	7.04 (d, 8.6)	6.97 (d, 8.5)	6.43 (d, 8.6)	6.36 (d, 8.7)	6.72 (d, 8.4)	6.72 (d, 8.6)	6.79 (d, 8.5)	6.86, overlapped	6.85, overlapped
6	7.42 (d, 8.6)	7.34 (dd, 8.5, 2.4)	7.00 (d, 8.6)	6.96 (d, 8.7)	7.17 (d, 8.4)	7.19 (d, 8.6)	7.21 (d, 8.5)	6.85, overlapped	6.85, overlapped
7	6.33 (d, 16.2)	6.29 (d, 16.3)	6.13 (d, 16.3)	6.11 (d, 16.2)	6.18 (d, 16.2)	6.25 (d, 16.2)	6.26 (d, 16.2)	6.19 (d, 16.2)	6.19 (d, 16.2)
8	6.20 (d, 16.2)	6.11 (d, 16.3)	5.95 (d, 16.3)	5.93 (d, 16.2)	5.99 (d, 16.2)	6.08 (d, 16.2)	6.09 (d, 16.2)	6.03 (d, 16.2)	6.03 (d, 16.2)
9									
10	1.53 (m)	1.50 (m)	1.45 (m)	1.45 (m)	1.46 (m)	1.49 (m)	1.50 (m)	1.46 (m)	1.46 (m)
11	1.98 (m)	1.96 (m)	1.92 (m)	1.91 (m)	1.93 (m)	1.94 (m)	1.95 (m)	1.93 (m)	1.93 (m)
12	5.12 (m)	5.10 (m)	5.09 (br t, 7.1)	5.08 (br t, 6.9)	5.08 (br t, 7.3)	5.10 (br t, 7.3)	5.10 (br t, 7.3)	5.09 (br t)	5.09 (br t)
13									
14	1.60 (s)	1.58 (s)	1.57 (s)	1.66 (s)	1.56 (s)	1.58 (s)	1.58 (s)	1.57 (s)	1.57 (s)
15	1.68 (s)	1.67 (s)	1.66 (s)	1.56 (s)	1.66 (s)	1.67 (s)	1.67 (s)	1.67 (s)	1.67 (s)
16	1.23 (s)	1.20 (s)	1.15 (s)	1.14 (s)	1.15 (s)	1.19 (s)	1.19 (s)	1.17 (s)	1.17 (s)
17	5.87 (dd, 17.6, 11.0)	5.88 (dd, 17.4, 10.7)	5.84 (dd, 17.2, 10.8)	5.83 (dd, 17.2, 10.8)	5.84 (dd, 17.7, 10.7)	5.87 (dd, 17.5, 10.9)	5.87 (dd, 17.5, 10.8)	5.85 (dd, 17.6, 10.7)	5.85 (dd, 17.6, 10.7)
18a	5.04 (dd, 17.6, 1.3)	5.02 (dd, 17.4, 1.4)	4.97 (dd, 17.2, 1.4)	4.97 (dd, 17.2, 1.4)	4.96 (dd, 17.7, 1.3)	5.01 (dd, 17.5, 1.3)	5.01 (dd, 17.5, 1.3)	5.01 (dd, 10.7, 1.3)	5.01 (dd, 10.7, 1.3)
18b	5.08 (dd, 11.0, 1.3)	5.04 (dd, 10.7, 1.4)	5.00 (dd, 10.8, 1.4)	5.00 (dd, 10.8, 1.4)	5.00 (dd, 10.7, 1.3)	5.03 (dd, 10.9, 1.3)	5.02 (dd, 10.8, 1.3)	4.99 (dd, 17.6, 1.3)	4.99 (dd, 17.6, 1.3)
1'									
2'		7.26 (d, 2.4)	7.00 (d, 8.6)	7.01 (d, 8.7)	7.16 (d, 8.7)	7.24 (d, 8.5)	7.18 (d, 8.4)	7.19 (br d, 8.6)	7.16 (br d, 8.6)
3'	5.68 (s)		6.56 (d, 8.6)	6.56 (d, 8.7)	6.71 (d, 8.7)	6.77 (d, 8.5)	6.74 (d, 8.4)	6.73 (br d, 8.6)	6.77 (br d, 8.6)
4'									
5'		6.97 (d, 8.5)	6.56 (d, 8.6)	6.56 (d, 8.7)	6.71 (d, 8.7)	6.77 (d, 8.5)	6.74 (d, 8.4)	6.73 (br d, 8.6)	6.77 (br d, 8.6)
6'		7.34 (dd, 8.5, 2.4)	7.00 (d, 8.6)	7.01 (d, 8.7)	7.16 (d, 8.7)	7.24 (d, 8.5)	7.18 (d, 8.4)	7.19 (br d, 8.6)	7.16 (br d, 8.6)
7'	7.43 (s)	6.29 (d, 16.3)	2.89 (br dd, 11.7, 10.6)	2.96 (br dd, 11.7, 10.5)	5.17 (d, 2.2)	4.18 (d, 8.7)	4.30 (d, 3.0)	4.80 (d, 7.3)	4.91 (d, 6.1)
8'		6.11 (d, 16.3)	4.06 (d, 10.6)	4.05 (d, 10.5)	3.46 (d, 2.2)	3.96 (d, 8.7)	3.54 (d, 3.0)	3.97 (d, 7.3)	4.04 (d, 6.1)
9'									
10'a	2.60 (d, 18.7)	1.50 (m)	1.98 (m)	1.72 (m)	1.86 (m)	1.76 (m)	2.32 (m)	1.76 (m)	1.55 (m)
10'b	2.46 (d, 18.7)		1.56 (m)	1.64 (m)	1.62 (m)	1.76 (m)	1.49 (m)	1.30 (m)	1.44 (m)
11'a		1.96 (m)	1.79 (dd, 12.3, 3.3)	1.70 (dd, 11.8, 3.5)	1.93 (m)	1.74 (m)	1.85 (m)	1.93 (m)	1.83 (m)
11'b		1.96 (m)	1.55 (dd, 12.3, 3.3)	1.60 (dd, 11.8, 3.5)	1.88 (m)	1.74 (m)	1.85 (m)	1.82 (m)	1.83 (m)
12'		5.10 (m)	2.53 (dt, 12.3, 3.3)	2.47 (dt, 11.8, 3.5)	4.58 (m)	3.14 (m)	4.08 (dd, 3.0)	5.06 (m)	5.03 (m)
13'									
14'	1.78 (s)	1.58 (s)	4.57 (br s), 4.54 (br s)	4.58 (br s), 4.56 (br s)	4.95 (d, 1.3), 4.91 (d, 1.3)	0.82 (s)	1.11 (s)	1.58 (s)	1.57 (s)
15'	1.78 (s)	1.67 (s)	1.51 (s)	1.56 (s)	1.35 (s)	0.49 (s)	1.09 (s)	1.66 (s)	1.67 (s)
16'	1.44 (s)	1.20 (s)	1.04 (s)	1.30 (s)	1.10 (s)	1.10 (s)	1.17 (s)	0.62 (s)	1.07 (s)
17'	5.87 (dd, 10.6, 7.5)	5.88 (dd, 17.4, 10.7)	6.43 (dd, 17.2, 10.8)	5.83 (dd, 17.2, 10.8)	6.46 (dd, 17.7, 10.9)	6.15 (dd, 17.5, 10.9)	6.02 (dd, 17.5, 10.8)	5.84 (dd, 17.4, 10.8)	5.48 (dd, 17.7, 11.0)

Table 1 (continued)

Position	1	2	3	4	5	6	7	8	9
18'a	5.19 (br d, 3.9)	5.02 (dd, 17.4, 1.4)	5.20 (dd, 17.2, 1.4)	5.20 (dd, 17.2, 1.4)	4.81 (d, 1.6)	5.14 (dd, 17.5, 1.3)	5.05 (dd, 17.5, 1.3)		
18'b	5.16 (br d, 10.6)	5.04 (dd, 10.7, 1.4)	5.29 (dd, 10.8, 1.4)	5.29 (dd, 10.8, 1.4)	4.85 (d, 1.6)	4.99 (dd, 10.9, 1.3)	5.02 (dd, 10.8, 1.3)		
OCH ₃						3.04 (s)	3.16 (s)		

Table 2 ¹³C NMR (100 MHz, CDCl₃) data for compounds 1–9

Position	1	2	3	4	5	6	7	8	9
1	136.2, C	131.6, C	130.3, C	129.9, C	130.5, C	132.7, C	132.8, C	131.3, C	131.4, C
2	127.8, CH	123.4, CH	126.6, CH	126.4, CH	126.9, CH	126.3, CH	126.4, CH	113.7, CH	113.9, CH
3	121.4, CH	128.9, C	115.9, CH	116.3, CH	115.2, CH	123.7, CH	124.0, CH	143.7, C	143.4, C
4	152.0, C	152.1, C	159.7, C	159.4, C	157.0, C	155.3, C	154.3, C	143.0, C	143.0, C
5	121.4, CH	116.7, CH	115.9, CH	116.3, CH	115.2, CH	123.7, CH	124.0, CH	116.5, CH	116.4, CH
6	127.8, CH	127.6, CH	126.6, CH	126.4, CH	126.9, CH	126.3, CH	126.4, CH	119.5, CH	119.5, CH
7	125.9, CH	126.1, CH	126.6, CH	126.7, CH	126.5, CH	126.6, CH	126.7, CH	126.5, CH	126.6, CH
8	138.9, CH	136.7, CH	135.3, CH	135.1, CH	135.7, CH	136.5, CH	136.5, CH	136.1, CH	136.1, CH
9	42.7, C	42.6, C	42.4, C	42.4, C	42.5, C	42.5, C	42.5, C	42.5, C	42.5, C
10	41.2, CH ₂	41.2, CH ₂	41.3, CH ₂	41.3, CH ₂	41.2, CH ₂	41.2, CH ₂	41.2, CH ₂	41.3, CH ₂	41.3, CH ₂
11	23.2, CH ₂	23.2, CH ₂	23.3, CH ₂	23.2, CH ₂	23.5, CH ₂	23.2, CH ₂	23.2, CH ₂	23.2, CH ₂	23.2, CH ₂
12	124.6, CH	124.7, CH	124.8, CH	124.8, CH	124.8, CH	124.8, CH	124.8, CH	124.8, CH	124.8, CH
13	131.4, C	131.3, C	131.2, C	131.2, C	131.2, C	131.3, C	131.3, C	131.5, C	131.4, C
14	17.7, CH ₃	17.6, CH ₃	17.6, CH ₃	17.6, CH ₃	17.6, CH ₃	17.6, CH ₃	17.6, CH ₃	17.6, CH ₃	17.6, CH ₃
15	25.7, CH ₃	25.7, CH ₃	25.7, CH ₃	25.7, CH ₃	25.7, CH ₃	25.7, CH ₃	25.7, CH ₃	25.7, CH ₃	25.7, CH ₃
16	23.2, CH ₃	23.3, CH ₃	23.3, CH ₃	23.3, CH ₃	23.4, CH ₃	23.3, CH ₃	23.3, CH ₃	23.4, CH ₃	23.4, CH ₃
17	145.5, CH	145.8, CH	146.0, CH	146.0, CH	146.0, CH	145.9, CH	145.9, CH	145.9, CH	145.9, CH
18	112.3, CH ₂	112.0, CH ₂	111.7, CH ₂	111.7, CH ₂	111.8, CH ₂	111.9, CH ₂	111.9, CH ₂	113.9, CH ₂	111.8, CH ₂
1'	131.6, C	131.6, C	133.3, C	133.3, C	131.9, C	131.5, C	132.4, C	130.4, C	130.4, C
2'	163.8, C	123.4, CH	126.6, CH	129.9, CH	128.0, CH	130.6, CH	128.9, CH	129.8, CH	129.6, CH
3'	104.5, CH	128.9, C	114.7, CH	114.7, CH	115.7, CH	114.8, CH	114.8, CH	115.4, CH	115.2, CH
4'	180.4, C	152.1, C	153.6, C	153.6, C	154.8, C	154.1, C	154.7, C	156.1, C	156.0, C
5'	144.8, C	116.7, CH	114.7, CH	114.7, CH	115.7, CH	114.8, CH	114.8, CH	115.4, CH	115.2, CH
6'	146.8, C	127.6, CH	126.6, CH	129.9, CH	128.0, CH	130.6, CH	128.9, CH	129.8, CH	129.6, CH
7'	126.6, CH	126.1, CH	49.0, CH	48.1, CH	79.9, CH	82.9, CH	84.8, CH	77.4, CH	76.4, CH
8'	122.7, C	136.7, CH	89.1, CH	87.8, CH	83.1, CH	80.5, CH	83.8, CH	81.8, CH	81.4, CH
9'	43.5, C	42.6, C	43.5, C	42.5, C	39.0, C	38.6, C	39.2, C	43.0, C	43.6, C
10'	51.4, CH ₂	41.2, CH ₂	36.6, CH ₂	35.5, CH ₂	34.0, CH ₂	32.8, CH ₂	30.7, CH ₂	38.3, CH ₂	38.8, CH ₂
11'	204.2, C	23.2, CH ₂	27.9, CH ₂	27.2, CH ₂	23.2, CH ₂	20.5, CH ₂	20.3, CH ₂	22.2, CH ₂	22.2, CH ₂
12'	163.0, C	124.7, CH	51.0, CH	50.7, CH	76.0, CH	76.3, CH	78.4, CH	124.5, CH	124.6, CH
13'	37.7, C	131.3, C	147.0, C	146.9, C	144.6, C	82.0, C	82.7, C	131.6, C	131.3, C
14'	22.3, CH ₃	17.6, CH	111.9, CH ₂	112.0, CH ₂	111.5, CH ₂	20.9, CH ₃	24.2, CH ₃	17.5, CH ₃	17.5, CH ₃
15'	22.5, CH ₃	25.7, CH ₃	19.2, CH ₃	19.3, CH ₃	19.3, CH ₃	23.4, CH ₃	21.9, CH ₃	25.7, CH ₃	25.7, CH ₃
16'	23.9, CH ₃	23.3, CH ₃	28.7, CH ₃	17.1, CH ₃	24.3, CH ₃	24.0, CH ₃	23.3, CH ₃	19.9, CH ₃	17.4, CH ₃
17'	142.5, CH	145.8, CH	141.2, CH	147.5, CH	143.4, CH	146.7, CH	145.8, CH	141.9, CH	141.9, CH
18'	114.5, CH ₂	112.0, CH ₂	114.2, CH ₂	111.6, CH ₂	112.2, CH ₂	111.7, CH ₂	111.1, CH ₂	111.8, CH ₂	112.4, CH ₂
OCH ₃						55.1	56.8		

Table 3 ^1H NMR (400 MHz, CDCl_3 ; δ_{H} , J in Hz) data and ^{13}C NMR (100 MHz, CDCl_3) data for compounds **10–12**

Position	10		11		12	
	δ_{H} (J in Hz)	δ_{C}	δ_{H} (J in Hz)	δ_{C}	δ_{H} (J in Hz)	δ_{C}
1		134.9, C		130.3, C		131.4, C
2	7.27 (d, 8.6)	126.6, CH	7.25 (d, 8.7)	127.1, CH	7.20 (d, 8.7)	126.4, CH
3	6.93 (d, 8.6)	124.5, CH	6.82 (d, 8.7)	115.9, CH	6.79 (d, 8.7)	121.6, CH
4		153.5, C		158.2, C		154.7, C
5	6.93 (d, 8.6)	124.5, CH	6.82 (d, 8.7)	115.9, CH	6.79 (d, 8.7)	121.6, CH
6	7.27 (d, 8.6)	126.6, CH	7.25 (d, 8.7)	127.1, CH	7.20 (d, 8.7)	126.4, CH
7	6.28 (d, 16.3)	126.5, CH	6.25 (d, 16.2)	126.6, CH	6.25 (d, 16.3)	126.7, CH
8	6.12 (d, 16.3)	137.1, CH	6.04 (d, 16.2)	135.5, CH	6.06 (d, 16.3)	136.0, CH
9		42.6, C		42.5, C		42.5, C
10	1.49 (m)	41.2, CH_2	1.49 (m)	41.3, CH_2	1.49 (m)	41.3, CH_2
11	1.94 (m)	23.2, CH_2	1.95 (m)	23.2, CH_2	1.95 (m)	23.2, CH_2
12	5.12 (m)	124.8, CH	5.11 (br t, 7.1)	124.8, CH	5.11 (m)	124.8, CH
13		131.3, C		131.2, C		131.3, C
14	1.58 (s)	17.7, CH_3	1.57 (s)	17.6, CH_3	1.58 (s)	17.7, CH_3
15	1.67 (s)	25.7, CH_3	1.67 (s)	25.7, CH_3	1.67 (s)	25.7, CH_3
16	1.20 (s)	23.3, CH_3	1.19 (s)	23.4, CH_3	1.19 (s)	23.4, CH_3
17	5.88 (dd, 17.4, 10.8)	145.8, CH	5.88 (dd, 17.4, 10.7)	146.1, CH	5.87 (dd, 17.4, 10.7)	146.0, CH
18a	5.10 (dd, 17.4, 1.3)	111.9, CH_2	5.01 (dd, 17.4, 1.3)	111.8, CH_2	5.01 (dd, 17.4, 1.3)	111.9, CH_2
18b	5.04 (dd, 10.8, 1.3)		5.03 (dd, 10.7, 1.3)		5.03 (dd, 10.7, 1.3)	
1'	1.25 (s),	21.8, CH_3		45.3, C		80.2, C
2'		84.1, C	4.24 (dd, 8.3, 5.4)	86.2, CH	2.35 (ddd, 11.7, 9.1, 8.6')	40.5, CH
3'	1.26 (s)	26.3, CH_3	1.87 (dd, 12.9, 5.4), 1.65(m)	44.0, CH_2	1.86 (dd, 9.1, 6.1), 1.72 (dd, 9.1, 8.6)	30.7, CH_2
4'	2.31 (m)	53.7, CH		38.3, C		34.7, C
5'	4.01 (d, 9.0)	79.8, CH	1.58 (br d, 14.8)	50.1, CH	2.04 (ddd, 11.7, 9.1, 6.1)	44.9, CH
6'		47.8, C	1.39 (m), 1.49 (m)	20.9, CH_2	1.41 (m), 1.53 (m)	21.3, CH_2
7'	1.61 (m), 1.52 (m)	35.1, CH_2	1.38 (m), 1.16 (m)	33.2, CH_2	1.50 (m), 1.19 (m)	36.1, CH_2
8'	1.95 (m), 1.49 (m)	22.8, CH_2		34.7, C		39.2, C
9'	5.95 (dd, 17.6, 10.8)	146.7, CH	3.34 (br t, 2.6)	75.0, CH	3.50 (t, 4.7)	71.8, CH
10'a	5.03 (dd, 10.8, 1.3)	112.0, CH_2	2.03 (m),	27.2, CH_2	2.01 (dddd, 15.5, 12.5, 5.5, 3.0)	28.3, CH_2
10'b	5.02 (dd, 17.6, 1.3)		1.80 (dd, 14.1, 5.1)		1.78 (ddt, 15.5, 5.5, 3.0)	
11'a	1.10 (s)	17.2, CH_3	1.38 (m)	26.7, CH_2	1.71 (m)	37.5, CH_2
11'b			1.06 (m)			
12'			1.56 (br s), 1.02 (br s)	36.0, CH_2	1.64 (d, 16.4), 1.49 (d, 16.4)	42.1, CH_2
13'			0.94 (s)	25.7, CH_3	1.01 (s)	20.9, CH_3
14'			1.06 (s)	31.4, CH_3	1.00 (s)	30.3, CH_3
15'			0.95 (s)	28.4, CH_3	0.92 (s)	26.4, CH_3

400 MHz), see Table 3; ^{13}C NMR (CDCl_3 , 100 MHz), see Table 3; HRESIMS m/z 445.3080 $[\text{M} + \text{Na}]^+$ (calcd for $\text{C}_{29}\text{H}_{42}\text{O}_2\text{Na}$, 445.3083).

Bakuchiol ether B (**11**). Yellowish oils; $[\alpha]_{\text{D}}^{25} + 20.0$ (c 0.1, MeOH); UV (MeOH) λ_{max} (log ϵ): 206(4.50), 265(4.45) nm; IR (KBr) ν_{max} 3420, 2926, 2864, 1715, 1606, 1507, 1463, 1364, 1245, 1173, 969 cm^{-1} ; ^1H NMR (CDCl_3 , 400 MHz), see Table 3; ^{13}C NMR (CDCl_3 , 100 MHz), see Table 3; HRESIMS m/z 477.3713 $[\text{M} + \text{H}]^+$ (calcd for $\text{C}_{33}\text{H}_{49}\text{O}_2$, 477.3733).

Bakuchiol ether C (**12**). Yellowish oils; $[\alpha]_{\text{D}}^{25} + 30.0$ (c 0.1, MeOH); UV (MeOH) λ_{max} (log ϵ): 206(4.46), 263(4.42) nm; IR (KBr) ν_{max} 3420, 2952, 2927, 1710, 1604, 1505, 1452, 1375, 1241, 1171, 967 cm^{-1} ; ^1H NMR (CDCl_3 , 400 MHz), see Table 3; ^{13}C NMR (CDCl_3 , 100 MHz), see Table 3; HRESIMS m/z 475.3532 $[\text{M} - \text{H}]^-$ (calcd for $\text{C}_{33}\text{H}_{47}\text{O}_2$, 475.3576).

X-ray crystallographic analysis

The X-ray crystallographic experiments were carried out on a XtaLAB Synergy R, HyPix diffractometer with *CuK α* radiation. Crystallographic data (No. CCDC 1993852) of **1** have been deposited at the Cambridge Crystallographic Data Center.

Crystallographic data of **1**: $C_{72}H_{80}O_8$, $M=1073.36$, $a=13.2661(2)$ Å, $b=14.3761(2)$ Å, $c=31.3617(5)$ Å, $\alpha=90^\circ$, $\beta=90^\circ$, $\gamma=90^\circ$, $V=5981.13(18)$ Å³, $T=100$ K, space group $P2_12_12_1$, $Z=4$, μ (Cu $K\alpha$) = 0.599 mm⁻¹, Crystal size = $0.99 \times 0.4 \times 0.02$ mm³, 2θ range for data collection = 8.344 to 139.15826790° , 26,790 reflections measured, 10,867 independent reflections ($R_{int}=0.0431$, $R_{sigma}=0.0446$). The final R_I value was 0.0475 ($I > 2\sigma(I)$). The final wR (F^2) value was 0.1153 . Flack parameter = -0.02 (12).

ECD calculations

The calculation was performed by the Gaussian 16 software. Conformation analysis were proceeded with the MMFF94s molecular mechanics force field. Optimization of the stable conformers with a Boltzmann distribution over 1% was conducted by time-dependent density functional theory (TD-DFT) at the Cam-B3LYP/6-31+G(d,p) level for compounds **8** and **9**, with the CPCM model in MeOH. The ECD data was analysed by SpecDis v1.71 with the half-bandwidth no more than 0.3 eV. The final ECD spectra were obtained based on the Boltzmann-calculated contribution of each conformer.

Inhibition assay on NO production

RAW264.7 cells were maintained in DMEM containing 10% FBS, in a constant humidity atmosphere of 5% CO₂ and 95% air at 37 °C. The cells were cultivated at a density of 3×10^5 cells/mL for 24 h in 96-well culture plates. And then, the cells were stimulated with LPS (1 µg/mL) and treated with various concentrations (1.56–50.00 µM) of assay compounds. After exposure to the compounds for 24 h, MTT (20 µL, 5 mg/mL) was added to each well [14]. 4 h later, 100 µL of lysis solution (40 g SDS, 20 mL isopropanol, 0.4 mL concentrated HCl and 400 mL ddH₂O) was added to dissolve the formazan crystals. Absorbances at 490 nm were measured after 10 h by a Multiskan MK3 Automated Microplate Reader (Thermo-Labsystems, Franklin, MA, USA).

The RAW264.7 cells were grown at a density of 3×10^5 cells/mL in 96-well culture plates. After 24 h, the cells were stimulated with LPS (1 µg/mL) and treated with various non-cytotoxic concentrations of assay compounds. And then, the cell culture supernatant (100 µL) was collected and reacted with the same volume of Griess reagent (100 µL) for 15 min at room temperature [15].

The absorbance was determined at 540 nm. The experiments were performed in parallel for three times, and L-NIL was used as a positive control. IC₅₀ (half maximal inhibitory concentration) value of each compound was defined as the concentration (µM) that caused 50% inhibition of NO production.

Statistical analysis

Data were analyzed by SPSS statistics package v.20.0 (SPSS Inc., Chicago, IL, USA). Results were expressed as the mean \pm SD. Students't-test was used for Statistical significances calculation, and $p < 0.05$ was considered to be statistically significant.

Results

Phytochemical investigation on cHE fraction of 70% ethanol extract of *Psoraleae Fructus* resulted in twelve unrepresented bakuchiol dimmers (**1**–**12**) and five known compounds (**13**–**17**) (Fig. 1). Structures of these new compounds were assigned by NMR spectra and single crystal X-ray diffraction. Compounds **1**–**3**, **6**–**9**, and **13**–**17** could be detected from ultrasonic extraction of *Psoraleae Fructus* by LC/MS analysis, suggesting that these compounds were natural products (Additional file 1: Fig. S1).

Compound **1** was obtained as brown–red needle crystals (MeOH) with mp 114–116 °C. It had the molecular formula $C_{36}H_{40}O_4$, as established by HRESIMS at m/z 537.3004 $[M+H]^+$ (calcd for 609.3216). Compared with the NMR data (Tables 1 and 2) of bakuchiol [16], a side chain (3-ethenyl-3,7-dimethyl-1,6-octadienyl) and a *p*-disubstituted benzene ring in **1** were identical to that of bakuchiol. The ¹H NMR data of another side chain of compound **1** exhibited three methyl groups at δ_H 1.78 (3H, s), 1.78 (3H, s) and 1.44 (3H, s); a vinyl group at δ_H 5.87 (1H, dd, $J=10.6, 7.5$ Hz, H-17'), 5.19 (1H, br d, $J=3.9$ Hz, Ha-18'), and 5.16 (1H, br d, $J=10.6, Hb-18'$); two trisubstituted olefinic protons at δ_H 5.68 (1H, s) and 7.43 (1H, s); and one methylene group at δ_H 2.60 (1H, d, $J=18.7$ Hz, Ha-10') and 2.46 (1H, d, $J=18.7$ Hz, Hb-10'). The presence of an α,β -unsaturated ketone group was revealed by the band at 1692 cm⁻¹ in its IR spectrum, which was confirmed by the resonance at δ_C 180.4(s) in its ¹³C NMR spectrum. Comparison of the ¹³C NMR spectrum of **1** with those of bakuchiol, the chemical shifts of C-3 and C-5 were shifted downfield to δ_C 121.4, suggesting that this substituted group was connected to C-4 of bakuchiol moiety by an ether linkage. The full assignment of ¹H and ¹³C NMR resonances was supported by ¹H–¹H COSY, DEPT, HSQC and HMBC spectral analyses. The X-ray structure was shown in Fig. 2 and confirmed the absolute configuration of 9*S*,9'*S* for **1**. Thus, the structure of **1** was as shown in Fig. 1 and named bisbakuchiol M.

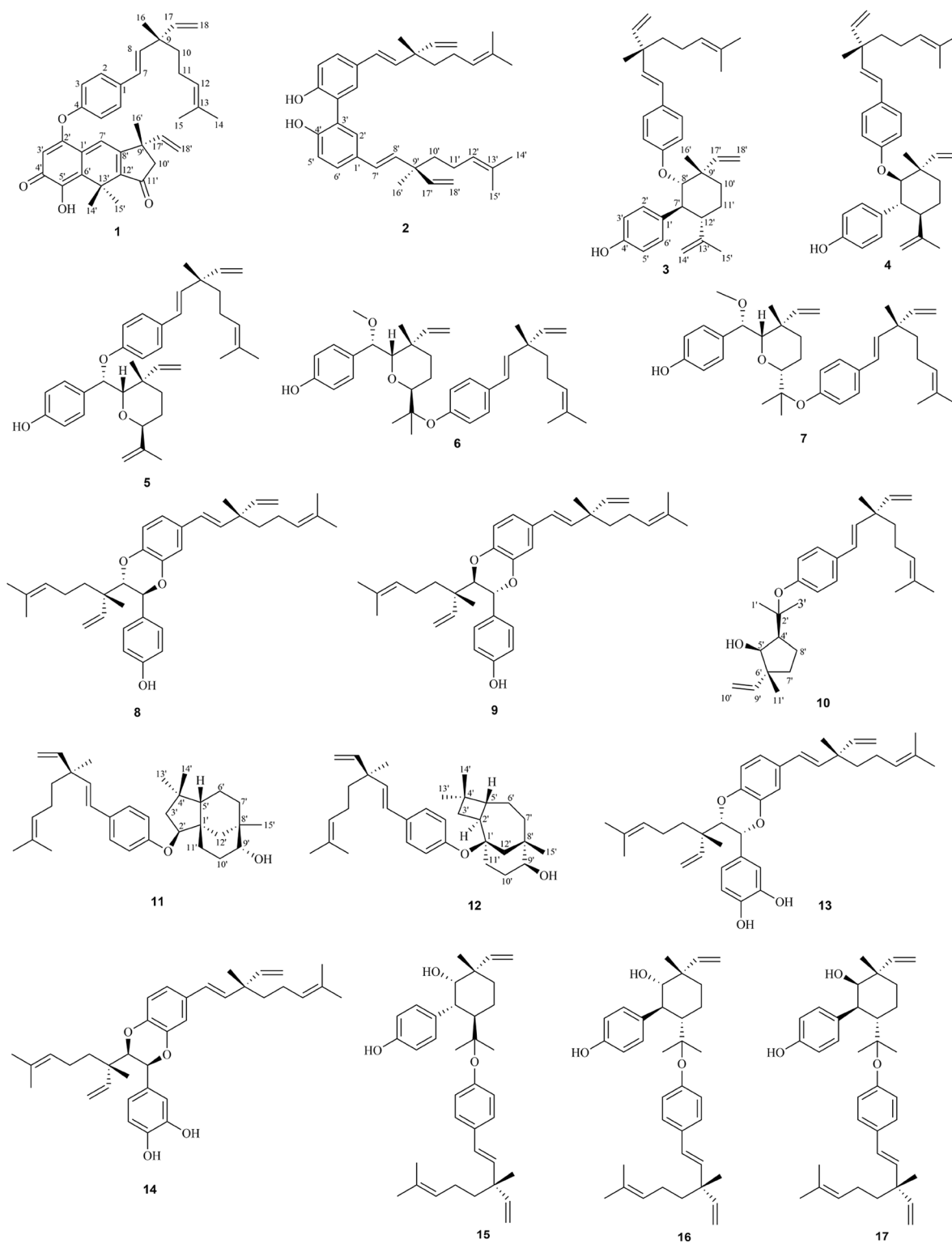


Fig. 1 Structures of compounds 1–17

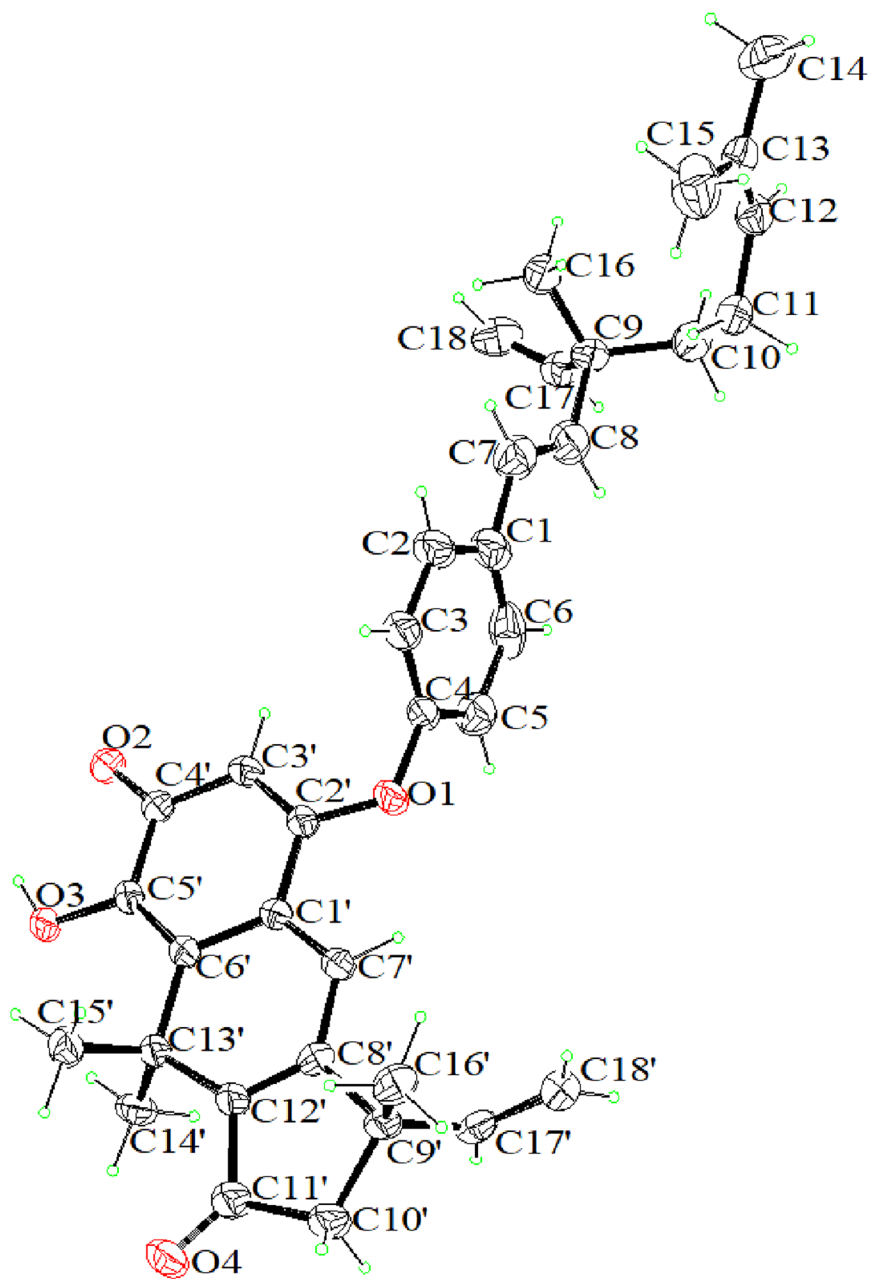
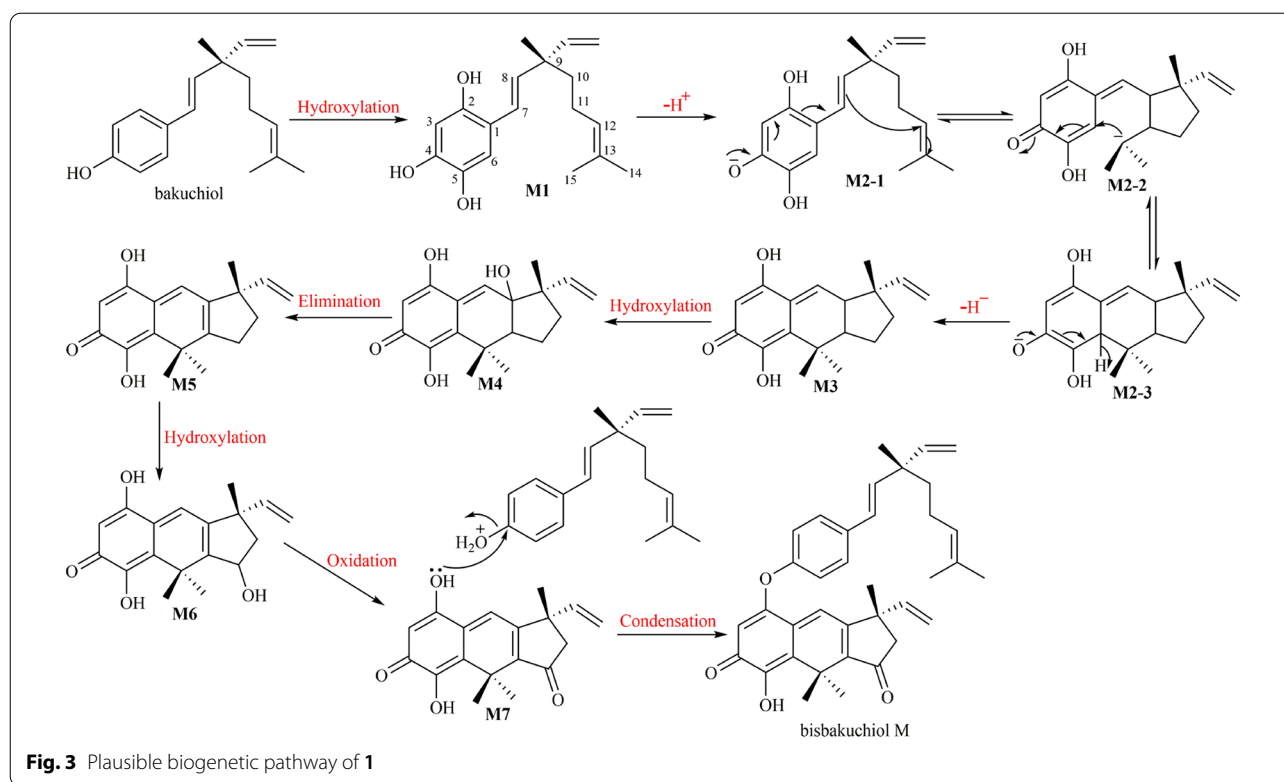


Fig. 2 X-ray ORTEP drawings of **1**

The plausible biosynthetic pathway of bisbakuchiol M was proposed (Fig. 3). Hydroxylation reactions occurred at the positions of C-2 and C-5 in bakuchiol to form M1. Once the 4-hydroxyl group in M1 lost a proton to generate M2-1, migrations of the double bond would start. The double bond at C-7 and C-8 would attack C-12 to form a five-membered ring, along with the generation of carbanion at C-13 (M2-2). Subsequently, the carbanion at C-13 attacked C-6 to form six-membered ring (M2-3). The

proton at C-6 left, which was accompanied by electron migrations of negative ion of oxygen to produce ketone carbonyl (M3). And then, the α -proton of double bond at C-8 was easily to be hydroxylated to generate M4. The elimination reaction would follow to the generation of M5. Similarly, the hydroxylation occurred at C-11 (M6). Subsequently, 11-hydroxyl group would be oxidized to ketone carbonyl (M7). Finally, M7 and bakuchiol were condensed to produce bisbakuchiol M.

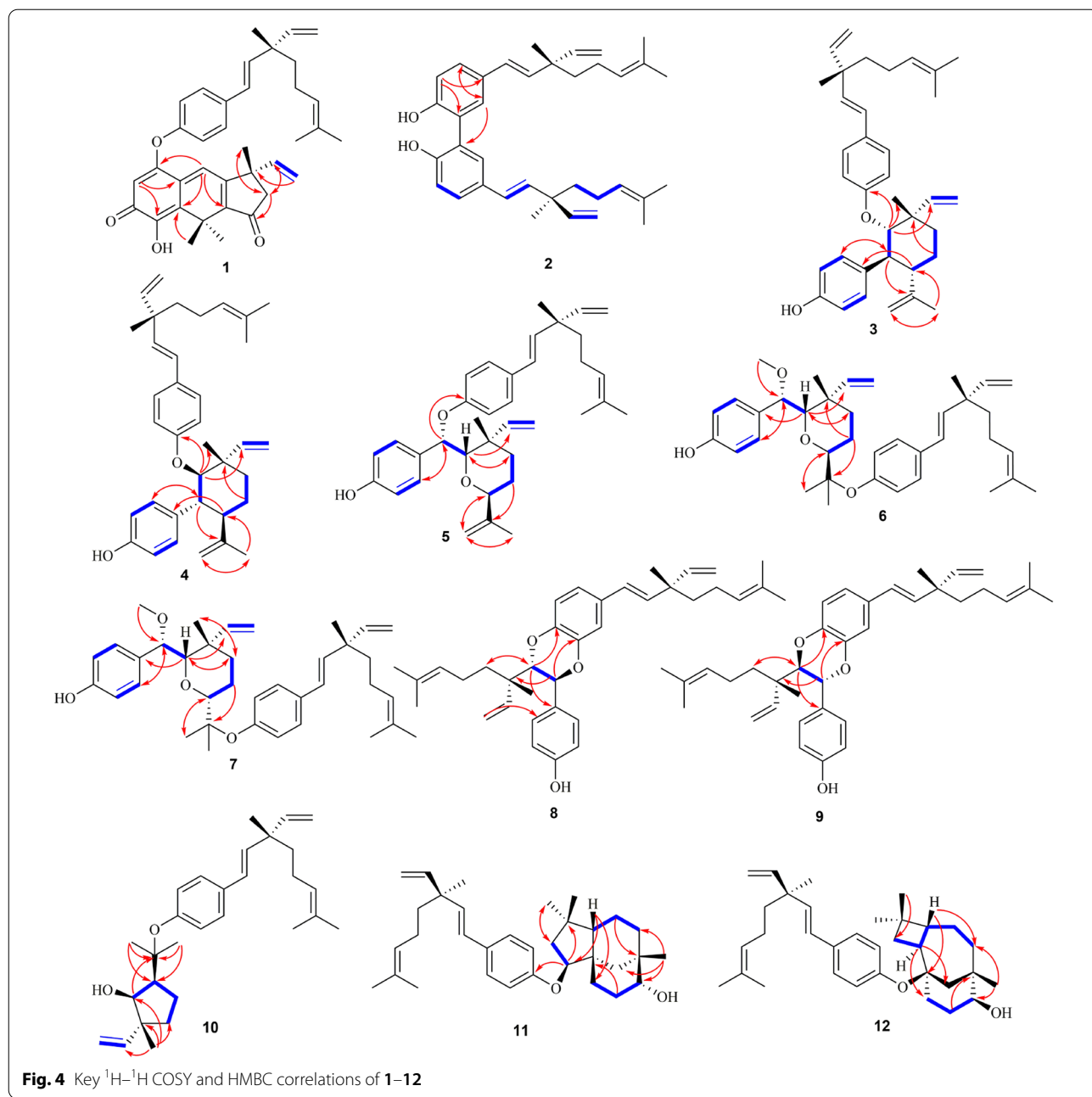


Compound 2 was isolated as yellow oils, had a molecular formula $C_{36}H_{46}O_2$ on the basis of the HRESIMS ion at m/z 511.3573 $[M+H]^+$. Compared with the NMR data of bakuchiol, a side chain in 2 was identical to that of bakuchiol. The resonances in the 1H NMR spectrum [δ_H 7.26, d, 2.4 Hz; 6.97, d, 8.5 Hz; and 7.34, dd, 8.5, 2.4 Hz] in 2 suggested clearly the 2,5,6-nature of the aromatic protons. Consequently, the structure of compound 2 was unambiguously identified as a dimer comprising two bakuchiol units by a C–C linkage, and it was given the trivial name bisbakuchiol N.

Compound 3 was isolated as yellowish oils with $[\alpha]_{25}^D + 30.0$, and possessed a molecular formula of $C_{36}H_{46}O_2$ by the HRESIMS ion at m/z 555.3468 $[M+HCOO]^-$. The IR spectrum of 3 showed absorption bands at 3373, 1604, 1507, 1454, 1238, 1007 cm^{-1} ascribable to hydroxyl group and ether functions and aromatic ring. Compared with the NMR data of bakuchiol, a side chain (3-ethenyl-3,7-dimethyl-1,6-octadienyl) and a *p*-disubstituted benzene ring in 3 were identical to that of bakuchiol, together with a set of remaining NMR signals, which were very similar to those of psoracorylifol F characterized from the fruits of *P. corylifolia* [17]. However, the NOE correlation between H-17' at δ_H 6.43 and H-7' at δ_H 2.89 was observed, which indicated that H-7' was α -oriented. The large coupling constant ($J=11.7$ Hz) of H-7' and H-12' indicated a *trans* configuration of the

two methine protons. Likewise, the configuration of H-8' was confirmed β -oriented on the basis of the large coupling constant ($J=10.6$ Hz). Thus, the configuration was assigned as $7'S,8'S,9'S,12'S$ from the occurrence of (9*S*)-bakuchiol only from nature [18, 19]. Furthermore, the HMBC cross-peaks of H-8' at δ_H 4.06 with aromatic C-4 at δ_C 159.7 indicated that C-8' was connected to C-4 of bakuchiol moiety by an ether linkage (Fig. 4). According to the above data, the structure of compound 3, named bisbakuchiol O, was established as shown in Fig. 1.

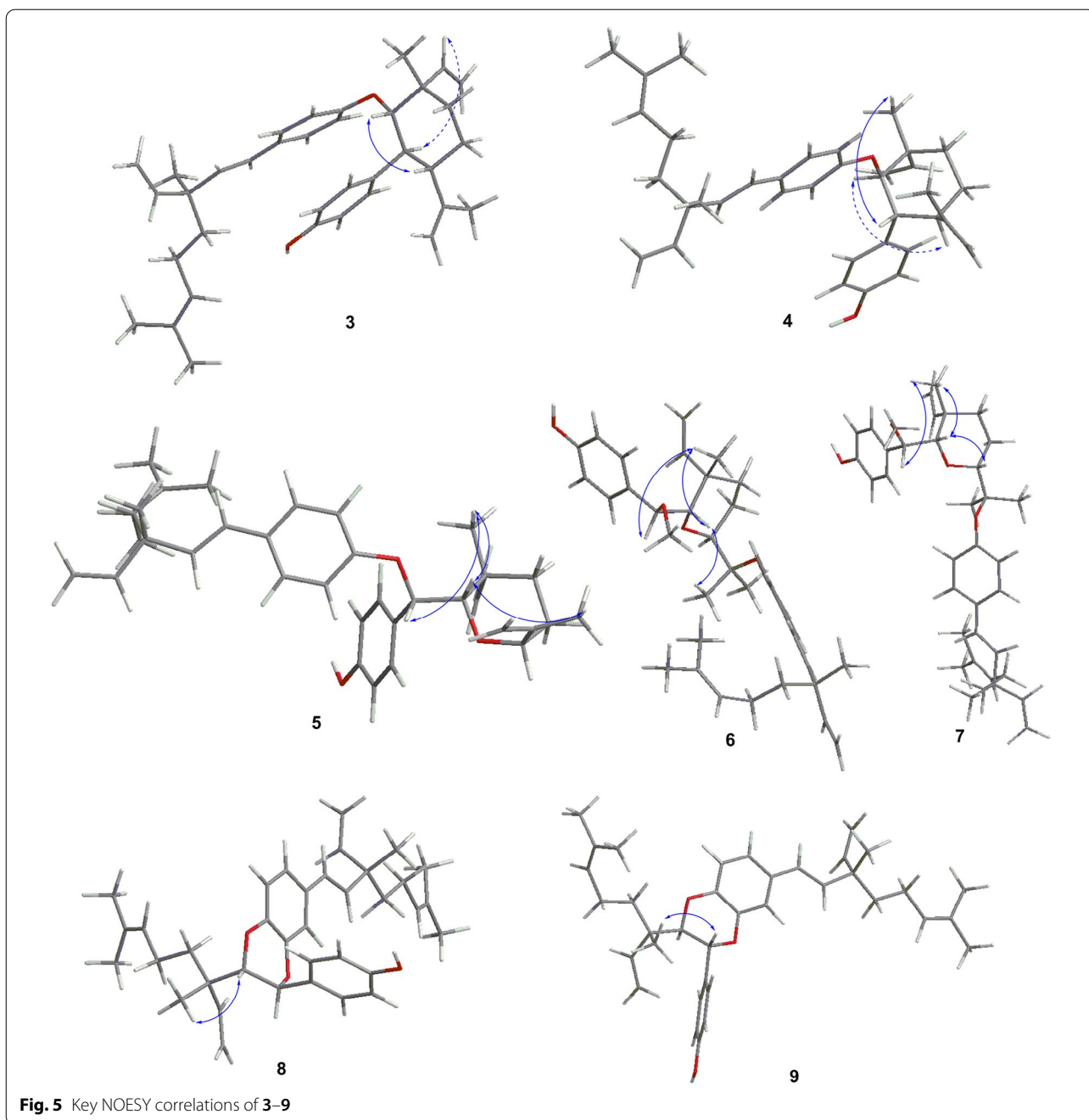
Compound 4 was also isolated as yellowish oils with $[\alpha]_{25}^D - 26.7$ (*c* 0.1, MeOH), and possessed the same molecular formula, $C_{36}H_{46}O_3$, as 3 according to the HRESIMS m/z 509.3417 $[M-H]^-$. Similarly, NMR data (Tables 1 and 2) for compound 4 was comparable to those of compound 3. Compared with compound 3, H-7' at δ_H 2.96 (1H, br dd, $J=11.7, 10.5$ Hz) displayed a NOE correlation with 16'-CH₃ at δ_H 1.30 (1H, s), indicating that they were cofacial, and H-7' was assigned in a β -configuration. And the large coupling constants ($J=11.7, 10.5$ Hz) indicated that H-8' and H-12' were α -oriented. As a result, the configuration was confirmed as $7'R,8'R,9'S,12'R$. According to the above data, compound 4 was a dimer, whose C-8' of psoracorylifol F was connected to aromatic C-4 of bakuchiol moiety by an ether linkage (Fig. 4). Thus, the structure of compound 4, named bisbakuchiol P, was established as shown in Fig. 1.



Compound 5 possessed the molecular formula of $\text{C}_{36}\text{H}_{46}\text{O}_3$ as determined by its HRESIMS ion at m/z 525.3364 $[\text{M}-\text{H}]^-$. Combined with NMR data, a set of bakuchiol unit signals except for downfield shift to δ_{C} 157.0 for C-4, and a set of psoracorylifol A unit signals [20] except for downfield shift to δ_{C} 79.9 for C-7' were observed. In the HMBC spectrum of 5 (Fig. 4), a psoracorylifol A unit located at C-4 of the bakuchiol unit was verified by correlations from H-7' at δ_{H} 5.17 to C-4 at δ_{C} 157. These features permitted assignment of the

planar structure of compound 5 as shown in Fig. 1. In the NOESY spectrum (Fig. 5), correlations between H-7' at δ_{H} 5.17 and CH_3 -16' β at δ_{H} 1.10, H-8' at δ_{H} 3.46 and CH_3 -16' β , indicated that H-7' and H-8' were β -oriented. Whereas H-12' at δ_{H} 4.58 was α -oriented, which was verified by the NOE correlation from H-8' and CH_3 -15' at δ_{H} 1.35. Thus, the absolute structure of compound 5, named bisbakuchiol Q, was established as 9*S*,7'*S*,8'*S*,9'*S*,12'*S*.

Compound 6 was isolated as white amorphous powders, and possessed the molecular formula of $\text{C}_{37}\text{H}_{50}\text{O}_4$



as deduced by HREIMS m/z 603.3676 $[M+HCOO]^-$. Similar NMR signals of bakuchiol and psoracorylifol A to 5 were observed in 6. In the HMBC experiment (Fig. 4), a characteristic methoxyl group at δ_H 3.04 (3H, s) correlated with C-7' enabled us to attach this methoxyl group to the C-7'. In NMR spectra of 6, the signals of an *exo*-methylene of psoracorylifol A unit had disappeared, while a new signal for characteristic methyl group at δ_H 0.49 (3H, s) and an oxygenated quaternary carbon at δ_C

82.0 had appeared. Combined with the downfield shift of C-3 and C-5 of bakuchiol unit, it was obvious that two units were attached together by C₄-O-C₁₃'. In the NOESY spectrum (Fig. 5), correlations between H-7' at δ_H 4.18 and CH₃-16'β at δ_H 1.10, H-8' at δ_H 3.96 and CH₃-16'β, indicated that they were cofacial and were β-oriented. Similarly, the NOE correlation between H-8' and CH₃-15' at δ_H 0.82 supported that H-12' at δ_H 3.14 was α-oriented. Finally, the structural assignment of 6

was assigned as 9*S*,7'*S*,8'*S*,9'*S*,12'*S*, and compound **6** was named bisbakuchiol R.

Compound **7** was isolated as white amorphous powders, and possessed the same molecular formula, $C_{37}H_{50}O_4$, as **6** according to the HRESIMS data (m/z 557.3635 $[M - H]^-$). Its 1D NMR pattern was highly overlapped to that of compound **6**, indicating their same planar structure. In the NOESY spectrum (Fig. 5), correlations between H-7' at δ_H 4.30, H-8' at δ_H 3.54, and CH_3 -16' β at δ_H 1.17 indicated that they were cofacial and were β -oriented. Meanwhile, the correlation between H-8' and H-12' at δ_H 4.08 suggested β -orientation of H-12'. Finally, the structural assignment of **7** was 9*S*,7'*S*,8'*S*,9'*S*,12'*R* as shown in Fig. 1 and compound **7** was named bisbakuchiol S.

Compound **8** was also isolated as yellowish oils with $[\alpha]_{25}^D -20.0$, and had a molecular formula of $C_{36}H_{46}O_3$ according to HRESIMS at m/z 525.3367 $[M - H]^-$ (calcd for $C_{36}H_{45}O_3$, 525.3369). Its NMR spectroscopic data (Tables 1 and 2) was consistent with those of a known bisbakuchiol A [21], except for the chemical shifts of B ring. A set of ABX type NMR signals had disappeared in bisbakuchiol A, whereas a set of A_2B_2 type NMR signals appeared at δ_H 7.19 (2H, br d, $J=8.6$ Hz, H-2', 6') and 6.73 (2H, br d, $J=8.6$ Hz, H-3', 5') in compound **8**. The configuration of **8** was elucidated through NOESY experiments (Fig. 5), where the correlation between H-8' at δ_H 3.97, and 16'- CH_3 at δ_H 0.62 suggested their same β -orientation. The coupling constant ($J=7.3$ Hz) between H-7' and H-8' confirmed a *trans* configuration of the two methine protons of the dioxane ring [21]. Thus, the configuration of **8**, named bisbakuchiol T, was established as 9*S*,7'*S*,8'*S*,9'*S*, which was supported by comparison of the calculated and experimental ECD curves (Fig. 6).

Compound **9** was isolated as yellowish oils with $[\alpha]_{25}^D +10.0$, and possessed the same molecular formula,

$C_{36}H_{46}O_3$, as **8** according to the HRESIMS data (m/z 525.3371 $[M - H]^-$). The 1H NMR and ^{13}C NMR spectral data (Tables 1 and 2) of **9** were quite superimposable with those of compound **8**, which clearly indicated the same skeleton as that of **8**. Likely, the NOE correlation between H-7' at δ_H 4.91 and 16'- CH_3 at δ_H 1.07, and the coupling constant ($J=6.1$ Hz) between H-7' and H-8', indicated that the configuration of **9** was 9*S*,7'*R*,8'*R*,9'*S*, which was consistent with ECD data (Fig. 6). Therefore, the structure of compound **9**, named bisbakuchiol U, was established as shown in Fig. 1.

Compound **10** was also isolated as yellowish oils. Its HRESIMS data exhibited a sodium adduct ion at m/z 445.3080 $[M + Na]^+$, establishing the molecular formula as $C_{29}H_{42}O_2$. Comparison of NMR spectra of **10** (Table 3) and known bakuchiol, a side chain (3-ethenyl-3,7-dimethyl-1,6-octadienyl) and a *p*-disubstituted benzene ring of **10** were identical to that of bakuchiol. In addition, the COSY, HSQC and HMBC correlations showed the presence of 2-ethenyl-2-methyl-5-isopropanol-cyclopentan-1-ol (6-ethenyl-6-methyl-4-isopropanol-cyclopentan-5-ol) substituted group in **10**. The chemical shifts of C-3 and C-5 in **10** were shifted downfield to δ_C 124.5, suggesting that this substituted group was connected to C-4 of bakuchiol moiety by an ether linkage. The relative configuration was mainly assigned by NOESY spectrum. The signals of H-4' at δ_H 2.31 and H-5' at δ_H 4.01 showed a NOE correlation, whereas H-4' or H-5' and 11'- CH_3 showed no correlation in its NOESY spectrum, indicating that both H-4' and H-5' were α -oriented. Therefore, the structure of compound **10**, named bakuchiol ether A, was defined as shown in Fig. 1.

Compound **11** showed a molecular formula of $C_{33}H_{48}O_2$ on the basis of the HRESIMS ion at m/z 477.3713 $[M + H]^+$. Similarly, compound **11** possessed a bakuchiol moiety by its NMR data. In addition, 2D NMR correlations in **11** showed the presence of clovane-2 β ,9 α -diol [22, 23] moiety with the exception of the resonances of C-1', C-2' to downfield shifts and C-3' and C-4' to high-field shifts. In the key HMBC spectrum (Fig. 4), the key correlation between H-2' at δ_H 4.24 and C-4 at δ_C 158.2 revealed that C-4 of bakuchiol moiety was connected to C-2' of clovane-2 β ,9 α -diol moiety by an ether linkage. Therefore, the structure of compound **11**, named bakuchiol ether B, was defined as shown in Fig. 1.

Compound **12** was isolated as yellowish oils with $[\alpha]_{25}^D +30.0$. It showed a molecular formula of $C_{33}H_{48}O_2$. The COSY, HSQC and HMBC correlations showed the presences of one set of the bakuchiol signals and one set of the caryolane-1,9 β -diol signals in compound **12** [23]. The chemical shifts of C-3 and C-5 were shifted downfield to δ_C 121.6 and the chemical shifts of C-1' was shifted downfield to δ_C 80.2 in **12**, suggesting that C-1'

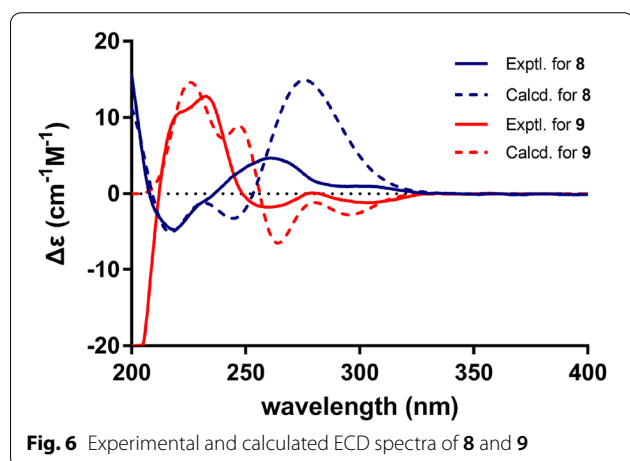


Fig. 6 Experimental and calculated ECD spectra of **8** and **9**

of this caryolane-1,9 β -diol moiety was connected to C-4 of bakuchiol moiety by an ether linkage. Therefore, the structure of compound **12**, named bakuchiol ether C, was defined as shown in Fig. 1.

Interestingly, when the quaternary carbon from the other unit was connected to bakuchiol unit by C–O–C₄, the chemical shifts of C-3 and C-5 would shift downfield (from 115 to 121 or 123 ppm) as shown in compounds **1**, **6**, **7**, **10**, **12**, **15**, **16** and **17**. Whereas, the link by CH–O–C₄ would not result in changes of chemical shifts at C-3 and C-5 as shown in compounds **3**, **4**, **5** and **11**. Therefore, we could infer the connection position of the dimers by the carbon chemical shifts of C-3/5 in bakuchiol unit.

NO, an unstable biological free radical, comes of *L*-arginine under the action of constitutive NO synthase (cNOS) and inducible NO synthase (iNOS). NO functions as a signaling molecule participating in neurotransmission and vasodilation. However, overproduction of NO is involved in inflammatory diseases, which can be treated by NO inhibitor. To evaluate their anti-inflammatory activities, compounds **1–17** (1.56–50.00 μ M) were tested for inhibition effect on NO production in LPS-stimulated RAW264.7 macrophages using the Griess reaction [15]. L-NIL, a selective inhibitor of iNOS, was used for the positive control. Firstly, the cytotoxicity of these compounds at concentrations from 1.56 to 50 μ M was assessed. The MTT tests demonstrated that compounds **4** and **16** showed cytotoxicity at the concentration of 50.00 μ M, whereas other compounds were not cytotoxic. The IC₅₀ values of these compounds were calculated at nontoxic concentrations. As shown in Table 4, compound **1** exhibited significant inhibition of NO production with IC₅₀ value at the concentration of 11.47 \pm 1.57 μ M, which showed no significant difference with that of L-NIL (10.29 \pm 1.10 μ M). Compounds **2**, **3**, **10–12**, **16** and **17** exhibited moderate inhibitory activities with IC₅₀ values at the range

of 15.98–27.80 μ M. The IC₅₀ values of the other compounds were more than 50.00 μ M, and they showed weak inhibitory activities against NO production.

Discussion

In our previous researches, we have obtained fourteen meroterpenoids and seventeen heterodimers of bakuchiol and evaluated their cytotoxicity [12, 13]. Further investigation on the cHE extract brought about 29 bakuchiol monomers and dimers, and their NO inhibition activities in LPS-stimulated RAW264.7 macrophages were studied. We have reported 9 monomers and 3 dimers in Chinese Traditional and Herbal Drugs [24]. In this research, seventeen bakuchiol dimers, including twelve unrepresented ones, were reported. Fortunately, a new skeleton bakuchiol dimer (**1**) was isolated, and it exhibited significant NO inhibition activities with IC₅₀ value of 11.47 μ M. Compounds **2**, **3**, **10–12**, **16** and **17** exhibited moderate inhibitory activities with IC₅₀ values at the range of 15.98–27.80 μ M, and other compounds showed weak inhibitory activity with IC₅₀ values more than 50.00 μ M.

In order to fully explore the relationship between structure and activity, results of 29 bakuchiol monomers and dimers were compared. Bakuchiol showed cytotoxicity at 12.50–50.00 μ M, and exhibited weak activity with inhibitory rate of 32% at the concentration of 6.25 μ M. Interestingly, structural changes at the side chain, including oxidation, cyclization and dimerization, reduced cytotoxicity. We found that the activities of uncyclized bakuchiol derivants seemed to be superior to cyclized ones. Notably, some uncyclized monomers and dimers with oxygen substitution at C-12/12' showed stronger inhibitory activities than L-NIL, such as 12,13-dihydro-12,13-epoxybakuchiol, 12-oxobakuchiol and (12'S)-bisbakuchiol C. Among dimers, compound **1** and (12'S)-bisbakuchiol C had excellent activities, which were mostly contributed by the 6/6/5 tricyclic ketone unit and the 12,13-dihydro-12,13-dihydroxybakuchiol unit respectively. And it was worth to mention that compounds (**3**, **16** and **17**) with a psoracorylifol F unit possessed better inhibitory activities than ones (**5–7**) with a psoracorylifol A unit.

Conclusion

Seventeen bakuchiol dimers (**1–17**), including 12 undescribed dimers and 5 known compounds, were isolated from the fruits of *Psoralea corylifolia* L. and their structure were identified by spectral methods and X-ray single-crystal diffraction. Bisbakuchiol M (**1**), whose other bakuchiol unit was cyclized to form a 6/6/5 tricyclic system, was a new skeleton compound. And the plausible

Table 4 Inhibition of **1–3**, **10–12** and **16–17** on NO production

Compound	IC ₅₀ (μ M)
1	11.47 \pm 1.57
2	23.52 \pm 1.82
3	21.43 \pm 2.04
10	27.80 \pm 1.18
11	26.86 \pm 1.05
12	23.54 \pm 0.82
16	15.98 \pm 2.30
17	24.93 \pm 1.13
L-NIL	10.29 \pm 1.10

biosynthetic pathway of bisbakuchiol M was proposed. Their inhibition on NO production in LPS-stimulated RAW264.7 macrophages were evaluated by the Griess reaction. Compounds **2**, **3**, **10–12**, **16** and **17** exhibited inhibitory activities, and the inhibition of compound **1** was equal to that of L-NIL. Their structure–activity relationship was discussed, showed that uncyclized monomers and dimers with oxygen substitution at C-12/12' showed strong inhibitory activities. And carbonyl units contributed to enhanced activities. These findings suggested that *Psoraleae Fructus* provided natural anti-inflammatory constituents and were of great significance in the design for anti-inflammatory drug.

Abbreviations

TCM: Traditional Chinese medicine; NO: Nitric oxide; IC₅₀: Half maximal inhibitory concentration; CC: Open column chromatography; TLC: Thin layer chromatography; RP-SP-HPLC: Reversed phase semi-preparative HPLC; PE: Petroleum ether; CHE: Cyclohexane; EtOAc: Ethyl acetate; DMEM: Dulbecco's modified Eagle's medium; FBS: Fetal bovine serum; CHCl₃: Chloroform; BuOH: Normal-butanol; MTT: 3-(4,5-Dimethyl-2-thiazolyl)-2,5-diphenyl-2H-tetrazolium bromide; LPS: Lipopolysaccharide; DMSO: Dimethylsulfoxide; L-NIL: L-N⁶-(1-iminoethyl)-lysine.

Supplementary Information **Additional file 1. Fig. S1.** MRM chromatogram (A: reference solution, B: test solution) for compounds 1–3, 6–9, and 13–17.

Acknowledgements

Not applicable.

Authors' contributions

XWY and YTZ designed the experiments. QXX and QL were responsible for isolation experiment. QXX finished biological activity assay. LL performed LC/MS analysis. XWY and QXX wrote the manuscript. All authors read and approved the final manuscript.

Funding

This work was supported by the National Natural Science Foundation of China (81773865).

Availability of data and materials

All data included in this article are available from the corresponding author upon request.

Declarations

Ethics approval and consent to participate

Not applicable.

Consent for publication

All authors have provided consent for publication in the journal of Chinese Medicine.

Competing interests

The authors declare no conflict of interest.

Received: 13 July 2021 Accepted: 31 August 2021

Published online: 07 October 2021

References

1. Ai TM. Medicinal Flora of China. Beijing: Peking University Press; 2016. p. 585–8.
2. Chinese Pharmacopoeia Commission. Pharmacopoeia of the People's Republic of China. Beijing: Chinese Medical Science and Technology Press; 2015. p. 187–8.
3. Chino M, Sato K, Yamazaki T, Maitani T. Constituent of natural food additive hokosshi extract and an analytical method for the additive in foods. *Shokuhin Eiseigaku Zasshi*. 2002;43(6):352–5.
4. Chopra B, Dhingra AK, Dhar KL. *Psoralea corylifolia* L. (Buguchi)—folklore to modern evidence: review. *Fitoterapia*. 2013;90:44–56.
5. Zhang XN, Zhao WW, Wang Y, Lu JJ, Chen XP. The chemical constituents and bioactivities of *Psoralea corylifolia* Linn.: a review. *Am J Chin Med*. 2016;44(1):35–60.
6. Lim SH, Ha TY, Kim SR, Ahn J, Park HJ, Kim S. Ethanol extract of *Psoralea corylifolia* L and its main constituent, bakuchiol, reduce bone loss in ovariectomised Sprague–Dawley rats. *Br J Nutr*. 2009;101(7):1031–9.
7. Kim YJ, Lim HS, Lee J, Jeong SJ. Quantitative analysis of *Psoralea corylifolia* Linne and its neuroprotective and anti-neuroinflammatory effects in HT22 hippocampal cells and BV-2 microglia. *Molecules*. 2016;21(8):1076.
8. Xin ZL, Wu X, Ji T, Xu BP, Han YH, Sun M, Jiang S, Li T, Hu W, Deng C, Yang Y. Bakuchiol: a newly discovered warrior against organ damage. *Pharmacol Res*. 2019;141:208–13.
9. Lin X, Li BB, Zhang L, Li HZ, Meng X, Jiang YY, Lee HS, Cui L. Four new compounds isolated from *Psoralea corylifolia* and their diacylglycerol acyltransferase (DGAT) inhibitory activity. *Fitoterapia*. 2018;128:130–4.
10. Sun NJ, Woo SH, Cassidy JM, Snapka RM. DNA polymerase and topoisomerase II inhibitors from *Psoralea corylifolia*. *J Nat Prod*. 1998;61(3):362–6.
11. Gao HTY, Lang GZ, Zang YD, Ma J, Yang JZ, Ye F, Tian JY, Gao PP, Li CJ, Zhang DM. Bioactive monoterpene phenol dimers from the fruits of *Psoralea corylifolia* L. *Bioorg Chem*. 2021;112:104924.
12. Xu QX, Zhang YB, Liu XY, Xu W, Yang XW. Cytotoxic heterodimers of meroterpenic phenol from the fruits of *Psoralea corylifolia*. *Phytochemistry*. 2020;176:112394.
13. Xu QX, Xu W, Yang XW. Meroterpenoids from the fruits of *Psoralea corylifolia*. *Tetrahedron*. 2020;76:131343.
14. MosMann T. Rapid colorimetric assay for cellular growth and survival: application to proliferation and cytotoxicity assays. *J Immunol Methods*. 1983;65:55–63.
15. Cao GY, Xu W, Yang XW, Gonzalez FJ, Li F. New neolignans from the seeds of *Myristica fragrans* that inhibit nitric oxide production. *Food Chem*. 2015;173:231–7.
16. Labbe C, Faini F, Coll J, Connolly JD. Bakuchiol derivatives from the leaves of *Psoralea glandulosa*. *Phytochemistry*. 1996;42(5):1299–303.
17. Xiao GD, Li XK, Wu T, Cheng ZH, Tang QJ, Zhang T. Isolation of a new meroterpene and inhibitors of nitric oxide production from *Psoralea corylifolia* fruits guided by TLC bioautography. *Fitoterapia*. 2012;83(8):1553–7.
18. Banerji A, Chintalwar GJ. Biosynthesis of bakuchiol, a meroterpene from *Psoralea corylifolia*. *Phytochemistry*. 1983;22(9):1945–7.
19. Takano S, Shimazaki Y, Ogasawara K. Enantiocontrolled synthesis of natural (+)-bakuchiol. *Tetrahedron Lett*. 1990;31:3325–6.
20. Yin S, Fan CQ, Dong L, Yue JM. Psoracorylifols A–E, five novel compounds with activity against *Helicobacter pylori* from seeds of *Psoralea corylifolia*. *Tetrahedron*. 2006;62:2569–75.
21. Wu CZ, Cai XF, Dat NT, Hong SS, Han AR, Seo EK, Hwang BY, Nan JX, Lee D, Lee JJ. Bisbakuchiols A and B, novel dimeric meroterpenoids from *Psoralea corylifolia*. *Tetrahedron Lett*. 2007;48(50):8861–4.
22. Wang AX, Zhang Q, Jia ZJ. A new furobenzopyranone and other constituents from *Anaphalis lacteal*. *Pharmazie*. 2004;59(10):807–11.
23. Heymann H, Tezuka Y, Kikuchi T, Supriyatna S. Constituents of *Sindora sumatrana* MIQ. III. New trans-clerodane diterpenoids from the dried pods. *Chem Pharm Bull*. 1994;42(6):138–46.
24. Lv Q, Xu QX, Zhang YT, Yang XW. Inhibition of bakuchiol and its derivatives in *Psoraleae Fructus* on nitric oxide production in lipopolysaccharide-activated RAW 264.7 cell lines. *Chin Tradit Herb Drugs*. 2020;51(2):307–14.

Publisher's Note

Springer Nature remains neutral with regard to jurisdictional claims in published maps and institutional affiliations.